Received: 19 November 2014 | Accepted: 17 October 2016

DOI 10.1002/hyp.11064

WILEY

RESEARCH ARTICLE

Hydrological responses to climatic variability in a cold agricultural region

Taufique H. Mahmood[4,1,2] | **John W. Pomeroy**[2,1] | **Howard S. Wheater**[1,2,3] | **Helen M. Baulch**[1,2,3]

[1] Global Institute of Water Security, University of Saskatchewan, Saskatoon, Saskatchewan, S7N 5C8, Canada

[2] Centre for Hydrology, University of Saskatchewan, Saskatoon, Saskatchewan, S7N 3H5, Canada

[3] School of Environment and Sustainability, University of Saskatchewan, Saskatoon, Saskatchewan, S7N 3H5, Canada

[4] Harold Hamm School of Geology and Geological Engineering, University of North Dakota, Grand Forks, North Dakota 58202, USA

Correspondence
Taufique H. Mahmood, Harold Hamm School of Geology and Geological Engineering, University of North Dakota, Grand Forks, North Dakota 58202, USA.
Email: taufique.mahmood@engr.und.edu

Abstract

Extended severe dry and wet periods are frequently observed in the northern continental climate of the Canadian Prairies. Prairie streamflow is mainly driven by spring snowmelt of the winter snowpack, whilst summer rainfall is an important control on evapotranspiration and thus seasonality affects the hydrological response to drought and wet periods in complex ways. A field-tested physically based model was used to investigate the influences of climatic variability on hydrological processes in this region. The model was set up to resolve agricultural fields and to include key cold regions processes. It was parameterized from local and regional measurements without calibration and run for the South Tobacco Creek basin in southern Manitoba, Canada. The model was tested against snow depth and streamflow observations at multiple scales and performed well enough to explore the impacts of wet and dry periods on hydrological processes governing the basin scale hydrological response. Four hydro-climatic patterns with distinctive climatic seasonality and runoff responses were identified from differing combinations of wet/dry winter and summer seasons. Water balance analyses of these patterns identified substantive multiyear subsurface soil moisture storage depletion during drought (2001–2005) and recharge during a subsequent wet period (2009–2011). The fractional percentage of heavy rainfall days was a useful metric to explain the contrasting runoff volumes between dry and wet summers. Finally, a comparison of modeling approaches highlights the importance of antecedent fall soil moisture, ice lens formation during the snowmelt period, and peak snow water equivalent in simulating snowmelt runoff.

KEYWORDS

drought, frozen soil infiltration, prairie hydrology, rainfall runoff, snowmelt, sublimation

1 | INTRODUCTION

The highly variable, cold, sub-humid, continental climate of the Canadian Prairies leads to sequences of extremely dry and wet years as a manifestation of the climate variability of this region (e.g., Bonsal & Wheaton, 2005; Bonsal et al., 2011a; Bonsal, Aider, Gachon, & Lapp, 2013; Nkemdirim & Weber, 1999). The hydrological impacts of such extreme climatic variation on society and the economy are manifold as droughts restrict local water availability for farms, communities, and industry; and the wet periods impair agricultural production and can lead to extensive flooding (e.g., Brimelow et al., 2014). Droughts are linked with atmospheric circulation over the Canadian Prairies. For example, large-scale atmospheric features such as a quasi-stationary mid-tropospheric ridge impede atmospheric moisture supply from the major sources and restrict recycling of evapotranspiration (e.g., Bonsal & Lawford, 1999; Bonsal, Wheaton, Meinert, & Siemens, 2011b; Liu, Stewart, & Szetco, 2004; Raddatz, 2000; Shabbar, Bonsal, & Khandekar, 1997; Shabbar, Bonsal & Szeto, 2011). Canadian Prairie drought is commonly associated with warmer summers (Roberts, Stewart, & Lin, 2006), colder winters (Fang & Pomeroy, 2007; Stewart, Bonsal, Harder, Henson, & Kochtubajda, 2014), higher near-surface energy in summer, a smaller percentage of precipitation occurring under overcast conditions, intense precipitation events, lower annual precipitation, and sparse vegetation (Armstrong, Pomeroy, & Martz, 2015; Roberts et al., 2006; Stewart, Henson, Carmichael, Hanesiak, & Szetco, 2011). These extreme climate years exert strong controls on hydrological processes such as snow accumulation, runoff, frozen soil infiltration, and evapotranspiration (e.g., Pomeroy et al., 2011).

 Copyright © 2016 John Wiley & Sons, Ltd.

Several studies have been conducted to understand the impacts of drought and wet periods on prairie hydrological responses. The 1999–2005 drought resulted in a substantial reduction in spring runoff as a consequence of reduced snow accumulation and snowmelt (Fang & Pomeroy, 2007; Fang & Pomeroy, 2008; Pomeroy et al., 2011), combined with significant depletion of soil moisture due to the high evaporative loss (Armstrong, Pomeroy, & Martz, 2010; Armstrong et al., 2015; Brimelow & Hanesiak, 2011; Brimelow, Raddatz, & Hayashi, 2010a; Brimelow, Hanesiak, & Raddatz, 2010b). This extended drought event also caused marked declines in groundwater and surface water storage and led to wetland drying within the prairie pothole region (Marin, van der Kamp, Pietroniro, Davison, & Toth, 2010; Van der Kamp & Hayashi, 2001). However, amid the 1999–2005 drought, an extreme precipitation event in the summer of 2002 caused a major flood and subsequent high streamflow in southern Manitoba (Stewart et al., 2011).

In general, Canadian Prairie wet periods are associated with flooding either due to spring snowmelt over frozen soils or multiple days of heavy rainfall in summer (Brimelow et al., 2014; Government of Manitoba, 2009; Government of Manitoba, 2012). The Canadian Prairies have strongly fluctuating precipitation regimes, resulting in sequences of drought and wet climatic conditions (Brimelow et al., 2014). For example, during 2009 in southern Manitoba, heavy snowmelt runoff resulted in devastating flooding across the cities and towns of the Manitoba portion of the Red River basin with $40 million estimated damage (Government of Manitoba, 2009), whilst in the subsequent summer, a severe drought developed. In contrast, heavy rainfall persisting over several consecutive days caused severe and widespread flooding in 2005, 2010, 2011, and 2014 summers (e.g., Brimelow et al., 2014). Wet soils and inundated fields during wet periods can lead to extensive unseeded farmland area.

Comparing cold region hydrological processes during dry and wet climatic periods requires coordinated winter and summer observations over multi-year periods. Physically based models can be used to extrapolate limited field observations over broader spatiotemporal scales in order to investigate the hydrological controls. In the Canadian Prairies, overwinter wind redistribution of the seasonal snowpack, sublimation, spring snowmelt energetics, infiltration into frozen soils, fill and spill runoff formation, depressional storage dynamics, rainfall intensity, infiltration into unfrozen cultivated soils, evapotranspiration, subsurface storage dynamics, variable contributing areas for runoff generation, and intermittent streamflow typically control the land surface hydrological cycle (Pomeroy et al., 2007). Numerical representations of this cycle need to refer to the governing hydrological processes. The Cold Regions Hydrological Modeling (CRHM) platform (Pomeroy et al., 2007) is an object-oriented, multi-physics, modular modeling system that allows creation of hydrological models that represent key cold regions hydrological processes from a range of possible configurations and algorithm choices. CRHM models have been widely used and tested in various agricultural regions in Canada, as well as in other cold regions such as the Canadian Rockies, Qinghai-Tibetan Plateau, Patagonia, the Pyrenees, and the Alps (Ellis & Pomeroy, 2007; Ellis, Pomeroy, Brown, & MacDonald, 2010; Dornes, Pomeroy, Pietroniro, Carey, & Quinton, 2008; Fang et al., 2013; Lopez-Moreno, Pomeroy, Revuelto, & Vicente-Serrano, 2012; Rasouli, Pomeroy, Janowicz, Carey, & Williams, 2014).

To date, detailed studies of the impacts of dry and wet periods on hydrological processes have focused on responses in the semi-arid prairies of Saskatchewan (e.g., Fang & Pomeroy, 2007; Fang & Pomeroy, 2008; Fang et al., 2010), with limited work on the wetter sub-humid prairie basins of southern Manitoba (Liu, Yang, Yu, Lung, & Gharabaghi, 2015). The objective of this study is to investigate the hydrological contrast between wet and dry periods in a sub-humid agricultural basin and the controlling factors that define this contrast. To do this, CRHM is used to build a model of cold region agricultural hydrology processes, including a process structure, basin discretization, and parameterization that is consistent with hydrological process studies in the region and nearby.

2 | METHODS

2.1 | Study area

The South Tobacco Creek (STC) basin (~73 km^2) is located on the western flank of the Red River basin (~49.33 N, 98.35 W) in southern Manitoba, Canada (Figure 1a). Its prairie agricultural landscape is divided into uplands to the west of the Manitoba escarpment and the Manitoba lowland to the east (Figure 1a). The terrain gently slopes from west to east with low relief (~200 m) and an average elevation of ~427 m (Figure 1b). An intensive set of hydrometeorological observations and agricultural land surface characteristics were collected from 1991 to 2011 and make the basin attractive for detailed hydrological analysis (Liu, Elliott, Lobb, Flaten, & Yarotski, 2014a; Liu et al., 2014b; Tiessen et al., 2010; Tiessen et al., 2011). Spatial data characterizing the basin include the following: a Light Detection and Ranging (LIDAR)-based digital elevation model (DEM) at 5-m resolution (Figure 1b), a geographic information system model characterizing each agricultural field by crop type, seeding and harvest date, riparian forest and pasture (Figure 1c), and a soil texture map. Riparian forests cover ~24% of the basin, primarily around channels in the upland part of the basin, with crops covering most of the (~76%) upland and lowland areas. Wheat and canola are often rotated in the same fields over sequential years, and varying degrees of conservation tillage have been practiced in recent decades. However, Tiessen et al. (2010) reported no difference in runoff between conventional and conservation tillage under an unconstrained environment at field scale. The upland portion of the basin is dominated by agricultural fields while the lowland portion of the basin has both riparian forest and agricultural fields (Yang, Rousseau, & Boxall, 2007). Soil stratigraphy is characterized by A, B, and C horizons composed of clay loam, loam, and clay soil, respectively (based on field observations by Watershed Evaluation of Beneficial Management Practices project (WEBs project); Koiter et al., 2013). The bedrock below the soil layers is Cretaceous shale bedrock which is mainly from Pierre Shale and Niobrara Formations (Koiter et al., 2013). The shale bedrock is relatively low in strength and has low resistance to fluvial processes, which coupled with freeze thaw and

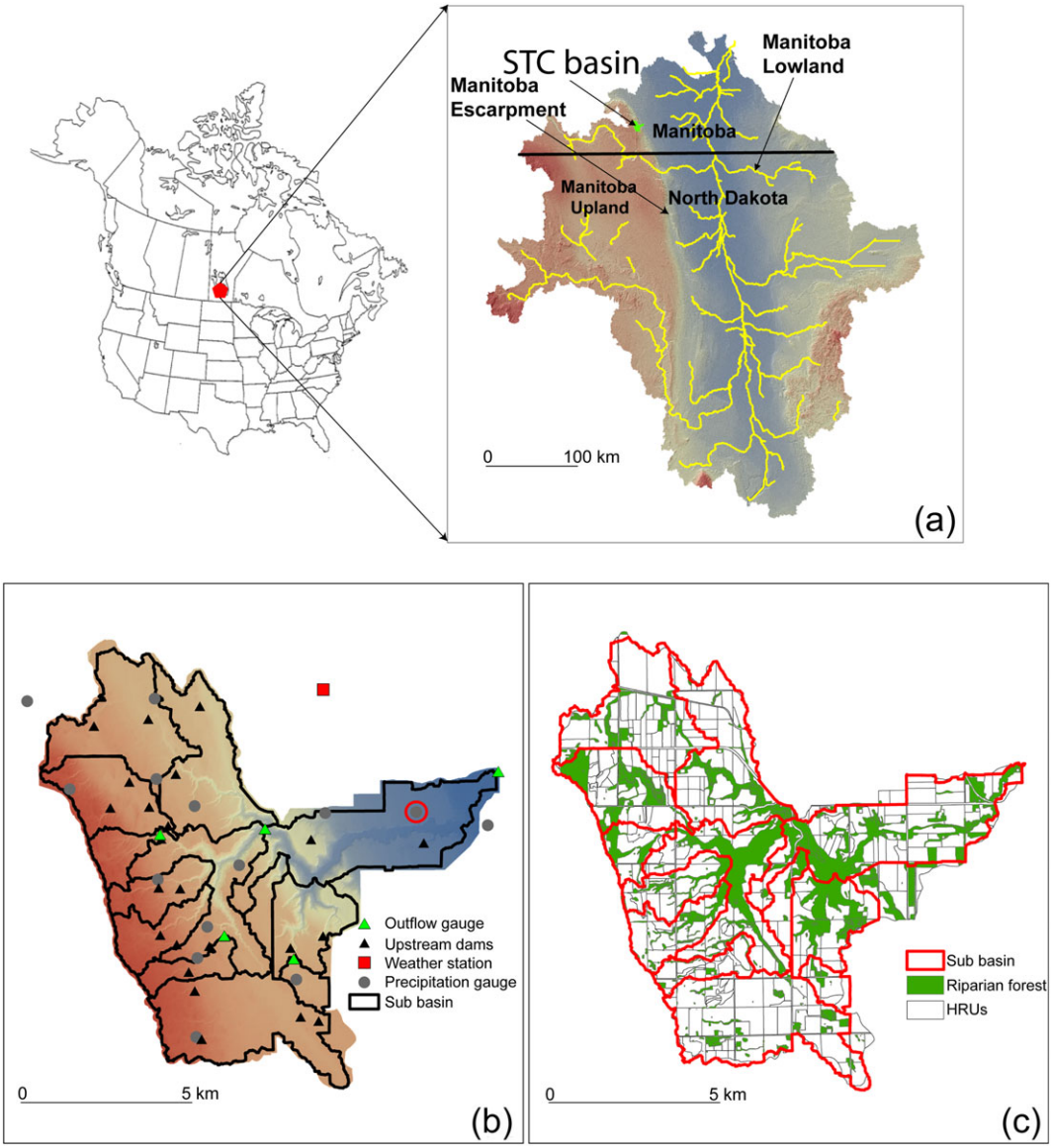

FIGURE 1 Location of the study site and hydrometeorological observatories and land surface properties: (a) location of the study site in the Red River Basin; (b) topography derived from Light Detection and Ranging digital elevation model and locations of precipitation gauges, streamflow measurement gauges, weather station, and upstream dams in the South Tobacco Creek (STC) basin; and (c) sub-basins, hydrological representative units (HRUs) within each sub-basin and riparian forest map of the STC basin. Note that in Figure 1b, the precipitation gauge (gray circle) circled by red line, only provide year-around precipitation while others are operated during spring and summer seasons

wetting and drying cycles results in rapid disintegration into fine-grained sediment (Koiter et al., 2013). Small dams and reservoirs, strategically constructed in the upstream sub-basins, are used to restrict agricultural runoff (Liu et al., 2014b). Because it is located in southern Manitoba, the STC basin is wetter (average annual precipitation: 550 mm) and warmer (average annual temperature: 4°C) than most of the Canadian Prairies (Liu et al., 2014b; Liu et al., 2015). Annual precipitation averages 590 and 500 mm above and below the Manitoba escarpment (e.g., Liu et al., 2014b) while mean temperature in the STC basin ranges from 2 to 4°C (Liu et al., 2014b). In addition, snowfall contribution to the annual precipitation is ~25%, and snowfalls generally occur from November to March. Based on long-term observations (1964–2010), average annual runoff is 69.4 mm of which 80% occurs during spring. There is very little base flow contribution to annual runoff (Liu et al., 2014b; Liu et al., 2015) suggesting that there is little connection between sub-surface storage and streamflow generation.

2.2 | Field observations

Hydrometeorological observations are available from an Environment and Climate Change Canada weather station, precipitation gauges at distributed locations and streamflow gauges at several locations along the main stream (Figure 1b). The dataset collected at STC included precipitation from Miami Orchard (Climate ID: 5021736, Environment and Climate Change Canada), Miami Thiessen (Climate ID: 5021737, Environment and Climate Change Canada), and a Twin watershed rainfall gauge and 12 rainfall gauges operated by local farmers. Air temperature, relative humidity, and wind speed were monitored at the Deerwood RCS station, (Climate

ID: 5020725) and snow depth observations are from the WEBs Project of Agriculture and Agri-food Canada. Both Miami Thiessen and Orchard stations are volunteer climate stations managed by Environment and Climate Change Canada, where snowfall is measured with a snow ruler and its water equivalent is estimated using an assumption that the density of fresh snowfall is 100 kg/m^3. No wind speed correction or gauge adjustment is needed for this type of observation. While the meteorological and runoff data were collected at hourly time steps, precipitation and snow observations were taken at daily intervals or longer. Only one Environment and Climate Change Canada precipitation gauge provided both winter and summer precipitation. Additional 12 gauges (Figure 1b) estimated only daily summer rainfall and were operated by local farmers (e.g., Yarotski & Rickwood, 2004; Yarotski & Rickwood, 2007). The precipitation gauge in the Twin basin (operated locally by Agriculture and Agri-food Canada and Environment and Climate Change Canada; the data are not available on the Environment and Climate Change Canada website; Figure 1b) provided hourly rainfall data during the summer period. The hourly rainfall distribution at the Twin sub-basin was used to distribute daily rainfall at an hourly time step for the whole STC basin. Working with the most comprehensive data available, the 2000–2011 period was considered for hydrological simulations.

Streamflow discharge measurements at an upstream sub-basin (sub-basin 2; ~2 km^2; WEBs project of Agriculture and Agri-food Canada), mid-basin at Hwy 240 (South Branch of STC near Highway 240, ~34 km^2, Water Survey of Canada, Station ID: 05OF023), and the basin outlet at Miami (STC near Miami, ~73 km^2, Water Survey of Canada, Station ID: 05OF017) as shown in Figure 1b provide opportunities for model evaluation at multiple scales. In the upstream sub-basin 2, the inflow and outflow of the basin outlet reservoir were estimated from water level measurements. Hydrometric gauging stations were used to estimate streamflow at Hwy 240 and Miami (Figure 1b). Generally, streamflow gauging starts when the ice in the channels begins to break up during spring (~March) and terminates when ice cover develops at the onset of winter (~October). The presence of snow and ice in the channels at the commencement of melting can lead to significant uncertainty in the early spring flow estimates.

Snow depth surveys were performed one to two times annually throughout the study period in two fields of a small, intensively studied basin (Twin basin, Figure 1b) downstream of the sub-basin 2 reservoir. Snow depth observations (Feb 2011) were available from sites in sub-basins 2, 11, 13, 7, 6, and 4. Snow depth was measured using a ruler. Snow depth measurements were taken when snow accumulation and ablation neared their peaks.

Figure 2 summarizes the hydrometeorological dataset used in this study, including the annual snowfall and rainfall contributions to precipitation, discharge of the STC basin at Miami, mean winter and summer air temperature for each water year (October 1 to September 30), and mean growing season (June 1 to September 30) relative humidity. Figure 2 shows significant interannual variability in annual precipitation and discharge. Annual precipitation varied from 395 to 630 mm with snowfall contributing approximately 30% to total precipitation (Table 1). Annual precipitation was low during 2002–2004 which also coincided with the extensive Canadian Prairie drought of 1999–2005.The first few years of the 2000s were dry in both winter and summer, with sustained low streamflow (water year 2001–2002, 2002–2003, and 2003–2004; Table 1). In contrast, the second half of the decade was wetter with moderate winter temperatures and high spring and summer precipitation. Mean winter temperature varied by almost 5.2°C between the coldest winter (−9.1°C in 2009) and the warmest winter (−4.1°C in 2006). However, the mean summer temperature varied very little over the study period. After 2004, annual precipitation increased substantially resulting in a wet period. Cumulative discharge rose in response to this precipitation shift, from 20 mm (2003) to 190 mm (2011; Figure 2), with substantial spring snowmelt and variable summer rainfall-runoff contributions (Table 1). Summer runoff measurements to runoff contributions were large during the 2002, 2005,

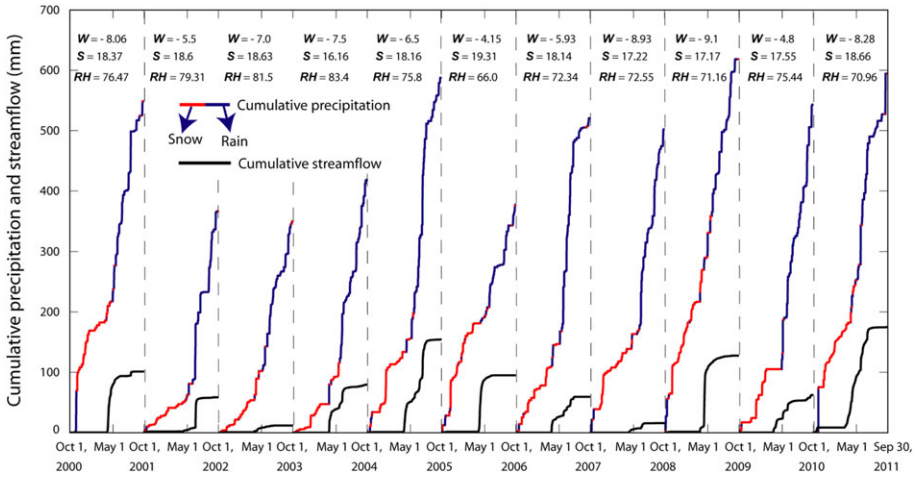

FIGURE 2 Hydrometeorological observations such as streamflow at the outlet gauge (Miami), cumulative precipitation with snow and rain component in the South Tobacco Creek basin. Note that black, red, and blue lines denote cumulative streamflow, snowfall, and rainfall. At the top of Figure 2, mean winter temperature (*W*), mean summer temperature (*S*), and mean relative humidity (*RH*) are written. Table 1 provides annual snowfall (mm), rainfall (mm), precipitation (mm), and streamflow at Miami gauge (mm) shown in Figure 2

TABLE 1 Annual snowfall (mm), rainfall (mm), precipitation (mm), and available streamflow (spring streamflow, summer streamflow) at Miami gauge (mm) for the South Tobacco Creek basin during 2001–2011 peiod

Year	Snowfall (mm)	Rainfall (mm)	Annual precipitation (mm)	Streamflow at Miami (mm; spring, summer)
2000–2001	140	408	548	102 (94, 8)
2001–2002	43	322	365	58 (13, 45)
2002–2003	88	261	349	13 (10, 3)
2003–2004	64	354	418	77 (70, 7)
2004–2005	110	477	587	155 (78.32, 77)
2005–2006	144	232	376	95 (95, 0)
2006–2007	93	427	520	60 (40, 20)
2007–2008	108	393	501	16 (6, 10)
2008–2009	204	414	618	128 (127, 1)
2009–2010	97	446	543	66 (36, 30)
2010–2011	134	460	594	175 (104, 71)

and 2011 periods. Interestingly, summer runoff was very small despite high summer rainfall during 2004, 2006, and 2009. As evapotranspiration, subsurface storage, and surface water storage are not measured, it is impossible to explain the fate of such high rainfall during 2002, 2004, and 2009 period from observations alone.

The observations in Table 1 have uncertainties and possible measurement errors. Snowfall observations at the Environment and Climate Change Canada volunteer stations might have site specific errors and errors due to the assumption of fresh snowfall density. The presence of snow and ice in stream channels at the beginning of snowmelt can lead to significant uncertainty in observations. Since the streamflow measurement starts in March, any runoff from mid-winter melt (~February) which can occur during warm winters (e.g., 2006) may be missing from the observation record.

2.3 | Hydrological simulations

2.3.1 | Modular structure

Models compiled in the CRHM platform can have a wide range of process structures with variable levels of complexity (Pomeroy et al., 2009). In the STC basin, a model representing cold region hydrological processes is required for realistic simulations. Figure 3 shows the schematic modules setup used for compiling the model.

1) Observation module: reads, adjusts, interpolates, and down-scales meteorological data such as air temperature, relative humidity, wind speed, and precipitation. The observation module was able to vary rainfall in space by providing rainfall input to respective hydrological response units (HRUs) from the nearest rain gauges. Inverse distance weighting was used to interpolate

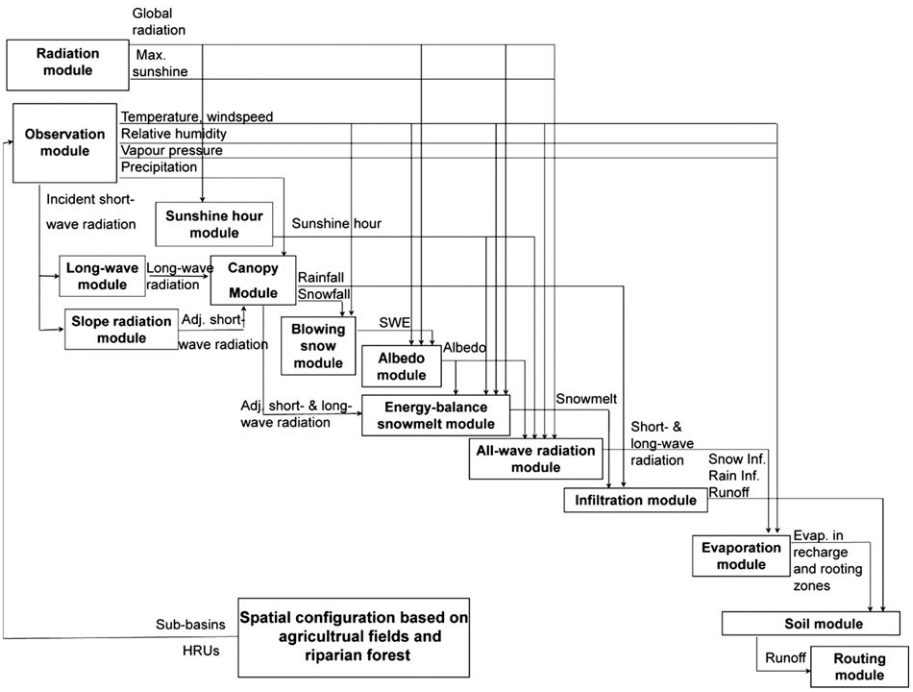

FIGURE 3 Flowchart of physically based hydrological modules utilized in the STC CRHM model

rainfall between stations outside the CRHM platform. These interpolated maps provided rainfall input to co-located HRUs. However, the inverse distance weighting interpolated rainfall did not improve model performance.

2) Radiation module: estimates the clear-sky direct and diffuse solar radiation based on latitude, elevation, ground slope, and azimuth (Garnier & Ohmura, 1970) and adjusts this for cloud cover based on incoming shortwave radiation estimated by the Annandale module.
3) Annandale module: estimates atmospheric transmittance from daily minimum and maximum temperatures using an empirical method developed by Shook and Pomeroy (2012) from one first developed by Annandale, Jovanic, Benade, and Allen (2002).
4) Longwave radiation module: estimates incoming long-wave radiation using temperature, humidity, and atmospheric short-wave transmittance (Sicart, Pomeroy, Essery, & Bewley, 2006).
5) Albedo module: calculates snow albedo through the winter and melt period and the non-snow albedo after snowcover depletion (Verseghy, 1991).
6) Canopy module: estimates interception of snowfall and rainfall by canopy and subsequent sublimation or release of intercepted snow by unloading or drip and evaporation or drip of rainfall from the canopy in order to estimate sub-canopy snowfall and rainfall. When there is a snowpack, sub-canopy shortwave and longwave radiation and turbulent fluxes to snow are calculated (Ellis et al., 2010, 2013; Pomeroy et al., 2009).
7) Blowing snow module: simulates the wind redistribution of snow between HRUs and in-transit blowing sublimation during the winter period (Pomeroy & Li, 2000; Fang & Pomeroy, 2009).
8) Energy balance snowmelt module: estimates snowmelt using the energy equation as its physical framework by estimating radiative, convective, advective and internal energy using semi-empirical techniques (Gray & Landine, 1987).
9) All-wave radiation module: estimates net radiation from shortwave radiation for the non-snow-covered period in order to calculate evapotranspiration (Granger & Gray, 1990).
10) Infiltration module: estimates infiltration into frozen and unfrozen soils. Frozen soils are classified as one of three classes: restricted, limited, and unlimited infiltration capacity. Restricted soils have impermeable layers such as ice lenses at or near the surface, limited soils permit infiltration to increase with snow water equivalent (SWE) and decrease with increasing frozen water saturation in the top 30 cm of soil, and unlimited soils allow all snowmelt to infiltrate assuming that a soil column has a high percentage of available pore spaces and macropores at the time of melt water release (Gray, Pomeroy, & Granger, 1986). For unfrozen soils, rainfall infiltrates at rates controlled by soil texture, depth to bedrock, and agricultural practice (Ayers, 1959).
11) Evaporation module: uses the Penman–Monteith combination method to estimate evapotranspiration (Monteith, 1965) by considering the influence of surface resistance (Jarvis, 1976; Verseghy, McFarlane, & Lazare, 1993) and available energy for evaporation and transpiration. Surface resistance varies as a function of plant growth status, vapor pressure deficit, soil moisture availability, and temperature at which transpiration can occur (Armstrong, Pomeroy, & Martz, 2008).
12) Soil module: estimates moisture balance, depressional storage, overland flow, and subsurface flow in two soil layers and a groundwater layer (Pomeroy et al., 2009; Dornes et al., 2008; Fang et al., 2010, 2013). The top soil layer receives infiltrated water from depressional storage, snowmelt, and rainfall and supplies water withdrawals by crop and tree roots for transpiration. The lower soil layer receives percolation from the recharge layer and supplies water for transpiration. This module limits evapotranspiration based on available interception, surface water storage, and soil water withdrawal characteristics.
13) Routing: utilizes the Muskingum routing method to transport from HRU to basin outlet (Chow, Maidment, & Mays, 1988). The routing module permits diversion of the outflow from one HRU to the inflow of other HRUs or to the basin or sub-basin outlet. Within a sub-basin, water from one HRU is diverted to downstream HRUs and ultimately routed to the outlet via the channel HRU. At the basin scale, the flow from each sub-basin is routed to the basin outlet.

2.3.2 | Spatial configuration

The STC model represents the basin using a distributed approach, discretizing the basin into HRUs. This level of spatial discretization is useful for modeling in basins where there is a good conceptual understanding of processes, but inadequate distributed information to characterize a basin at very fine scales, as is typical of fine scale gridded distributed models (Dornes et al., 2008). Each HRU is composed of modules representing important hydrological processes, based on results of other Canadian Prairie basin field and modeling studies (Pomeroy et al., 2007; Fang et al., 2010). The HRUs were derived from field-surveyed agricultural field, riparian forest, and pasture polygons. Elevation and slope were calculated for each HRU using a LiDAR-derived DEM. A total of 372 HRUs were distributed over 13 sub-basins (Figure 4). The semi-distributed simulation structure developed for the STC model is also shown in Figure 4. The outlets of sub-basins were identified using stream gauge locations in a contributing area map, and the sub-basin boundaries were delineated using a flow direction map. The ArcGIS Hydrology software package was used to produce the flow direction (Jenson & Domingue, 1988) and contributing area map (Tarboton, Bras, & Rodriguez–Iturbe, 1991) from the LIDAR DEM. One HRU simulated reservoir streamflow, using reservoir capacity and a rating curve. It was deployed for sub-basin 2, where a small reservoir had been constructed to attenuate the peak flow during the snowmelt period. Sub-basins 1, 2, 3, 4, 5, and 6 drain the Manitoba Escarpment from relatively higher elevations (436–500 m) with an average relief of 65 m. Sub-basins 7, 8, 9, 10, 11, and 12 drain mid-elevations (360–460 m) and have a high percentage of the STC riparian forest in sub-basins 9, 10, 11, and 12. Sub-basin 13 is low lying (306–404 m) and receives inflows from the 12 upstream sub-basins. Sub-basins 1, 2, 3, 4, 5, 6, and 12 drain to the Hwy 240 gauge, and all sub-basins drain to the Miami gauge via the flow network shown in Figure 4.

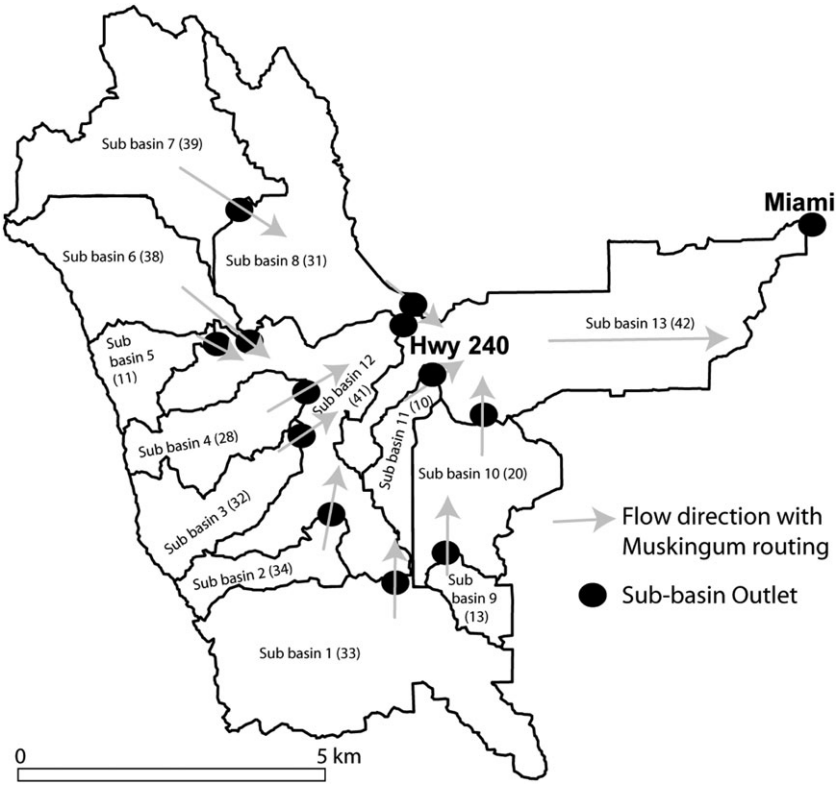

FIGURE 4 The spatially distributed modeling structure for the South Tobacco Creek basin. The 13 sub-basins are composed of various hydrological representative units (HRUs), and each HRU contains a set of physically based hydrological modules as its internal structure. Muskingum routing routes flow from non-channel HRUs to valley bottom HRU in each sub-basin and then from all 13 sub-basins (shown by the light gray lines with arrow that indicate flow direction)

2.3.3 | Model parameter estimation, initialization, and evaluation

Land surface parameters were derived from field-based observations and previous research findings (e.g., Fang & Pomeroy, 2007; Fang & Pomeroy, 2008; Fang & Pomeroy, 2007; Fang et al., 2010; Pomeroy et al., 2007; Pomeroy, Fang, Shook, & Whitfield, 2013). Field-derived data included reservoir storage, crop residue, crop type, seeding date, harvest date, and soil texture. A crop residue index was used to estimate stubble height for winter blowing snow calculations. The crop residue index was set as a function of the fall tillage practice. A crop residue index of 1 indicates conservation fall tillage whereas values of 0.8, 0.7, 0.6, and 0.5 indicate conventional fall tillage using the anhydrous rig (minimal cultivation), light duty cultivator, heavy duty cultivator, and tandem disc, respectively. Based on personal communications with local farmers, the stubble height varies from 12 to 45 cm. It was assumed for model parameterization purposes that the stubble heights are 20 and 1 cm for conservation tillage and conventional tillage fields, respectively.

During the growing season, the crop height and leaf area index (LAI) start increasing from seeding date and continue increasing until crop maturity, estimated as 2 weeks before harvest date. Both crop height and LAI are reset, to pre-growth stubble height and LAI at the harvest date, respectively. Crop growth rate (cm/day) and LAI growth rate (−/day) are set in such a way that both reach a maximum at the crop maturity date.

Initial conditions were obtained by running the model for three consecutive years (Oct 1, 1997 to Sep 30, 2000) prior to the onset of the simulation period. Meteorological data from the same stations were used for the initialization run using the same model setup. Average fall soil moisture was assumed and set as an initial condition for the 3-year initialization run. The initialization period has one dry year (1997–1998: 390-mm precipitation) and two consecutive wet years (1998–1999: 660 mm and 1999–2000: 520-mm precipitation) which suggests that after 3 years of model runs and multiple spin-ups, the STC model was attuned to STC climatic conditions. The subsurface soil moisture was quite still low at the end of spin-up period. Infiltration during the wet period had not overcome the soil moisture deficit. Since the simulated streamflow agrees well with observations at the Miami gauge during the spin-up period, there is confidence that the modeled initial subsurface storage condition was adequate for further simulation. Snow observations at the Twin basin during the entire simulation period, snow depth observations at the distributed locations during the winter of 2010–2011, and streamflow measurement at sub-basin 2, Hwy 240, and Miami gauge were used to evaluate model performance and assess its suitability for use in examining hydrological response to climate variability. The Nash–Sutcliffe efficiency (*NSE*), root mean squared error (*RMSE*), normalized RMSE (*NRMSE*), and mean bias were used to compare the simulations with observations. The *NSE* is defined using the following equation (Nash & Sutcliffe, 1970):

$$NSE = 1 - \frac{\sum_{k=1}^{n}(obs_k - Sim_k)^2}{\sum_{k=1}^{n}(obs_k - \mu_{obs})^2} \quad (1)$$

where obs_k and sim_k are observations and simulations at time k, the total number of simulation hour is n, and μ_{obs} is the mean of all observations.

The normalized mean bias is defined using Equation 2:

$$Normalized\ mean\ bias = \frac{\sum_{k=1}^{n}(obs_k - Sim_k)}{n \times Obs_{mean}} \quad (2)$$

where obs_k and Sim_k are observations and simulations at time k, the total number of simulation hours is n, and μ_{obs} is mean of all observations.

For sub-basin 2, streamflow performance was assessed based on reservoir outflow compared with the simulated streamflow from the reservoir HRU. Other streamflow simulations for the mid-basin scale and the entire STC scale were evaluated using Environment and Climate Change Canada gauged discharges. The Hwy 240 gauge (mid basin) discharge is a composite of streamflow from the upper six sub-basins (sub-basins 1 [10.8 km^2], 2 [2.08 km^2], 3 [3.38 km^2], 4 [3.22 km^2], 5 [2.08 km^2], and 6 [5.5 km^2]) and also local inflows from the sub-basin 12 (7.54 km^2; Figure 4) whilst the Miami gauge receives flow from the upper 12 sub-basins and the local inflows from the sub-basin 13 (Figure 4).

2.4 | Simulated snowmelt and rainfall runoff analyses

To explore simulated rainfall runoff generation mechanisms, the metric (*fr*) and the percent contribution by heavy rainfall days (≥25 mm/day) to seasonal rainfall depth were used. The threshold value of 25 mm/day was taken from Brimelow et al. (2014), where they reported that, in wet summers, heavy rainfall days (≥25 mm/day) accounted for up to 55% of seasonal rainfall.

Factors influencing snowmelt runoff generation were assessed by comparing simulated snowmelt runoff with runoff estimated using a simplified calculation method – employing equations of Granger, Gray, and Dyck (1984) for limited infiltration into unsaturated, uncracked frozen soils, but without consideration of the impact from redistribution of blowing snow as suggested by Pomeroy and Li (2000) and over-winter snow-soil ice layer formation as suggested by Gray et al. (1986). Comparison of the Granger et al. method with full CRHM simulations of blowing snow redistribution and sublimation, mid-winter melt, and rain-on-snow formation of ice layers on the frozen soils allows assessment of the importance of these processes. Granger et al. (1984) provided an equation to approximate snowmelt infiltration into fully frozen soils based on SWE and pre-winter degree of pore saturation (Θ_p). This is used in the Gray et al. (1986) algorithm that forms the basis of the infiltration module used in the CRHM model for STC. In CRHM, infiltration is classified as limited, restricted (by ice layers), and unlimited (due to cracks) following Gray, Dyck, and Granger (1984). The equation used in the simplified method only applies for what Gray et al. (1984) termed the "limited" case where there were no large macropores, cracks, or ice layers. The unlimited or restricted cases require a full hydrological model to estimate their occurence. The Granger et al. (1984) equation for estimating infiltration in the limited infiltration case is given below:

$$INF = 5\,(1 - \Theta_p)SWE^{0.584} \tag{3}$$

where *INF* (mm) is snowmelt infiltration in mm. Equation 3 was used to approximate snowmelt infiltration from climate information assuming the limited case. As *SWE* data were not available for the simplified method, winter snowfall was used instead of *SWE*, which assumes that snowfall is not melted, sublimated, or redistributed by wind over the winter. Θ_p was taken from simulated soil moisture in the preceding fall season and soil porosity estimated from texture using Brooks–Corey relationships. By subtracting *INF* from winter snowfall, theoretical snowmelt runoff was estimated from climate data. Note that Equation 3 predicts infiltration at a seasonal scale and is active when *SWE* is greater than 0.

3 | RESULTS AND DISCUSSION

3.1 | Snow model evaluation

The snow simulations were evaluated against snow depth observations at the Twin basin (~0.094 km^2) and HRUs distributed across the STC basin. Figure 5 compares the observed snow depth at a site in the Twin basin with simulated values for the corresponding HRU. The observed spatial variability across the Twin basin is represented by a vertical bar on the graph. The model performance in predicting snow depth is satisfactory for all winter seasons across a range of

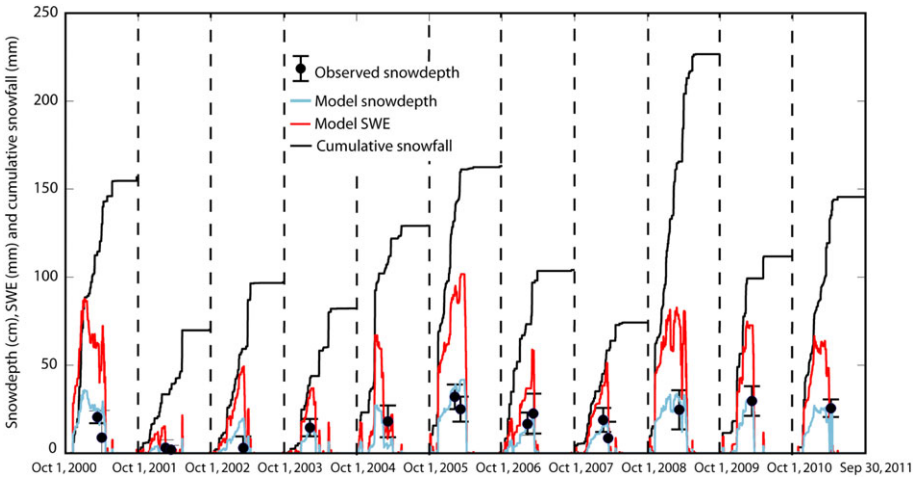

FIGURE 5 Comparisons between simulated and observed snow depths at the Twin basin inside the South Tobacco Creek basin during 2001–2011 period. Black circles represent mean observed snow depth, and vertical bars across the black circles represent ±1 standard deviation. Blue and red lines represent modeled snow depth (cm) and snow water equivalent (SWE in mm), respectively. Finally, black lines show cumulative snowfall in respective winters

different climatic (precipitation and temperature) conditions (Table 2), with an RMSE of 7.2 cm, NRMSE of 0.42, and normalized mean bias of −0.06. The model successfully captured the temporal dynamics of snow accumulation and ablation and performed well in capturing peak snow depth, indicating adequate modeling of winter snow redistribution and ablation due to blowing snow transport. The marked difference between cumulative snowfall and simulated peak SWE indicates significant winter snow redistribution, sublimation, and melt. CRHM model outputs show this is primarily due to snow erosion by wind transport rather than melt or direct sublimation from the snow surface. Figure 5 also shows marked variability in snowfall, peak SWE, and snow cover between winters. The simulation period starts with a series of dry winter years (2002–2004) of the major drought of 1999–2004, characterized by lower snow accumulation, shorter snow cover period, lower peak SWE, and even temporally discontinuous snow cover in 2002. In contrast, winters having high snowfall (2005, 2009, and 2011) show contrasting responses of greater snow accumulation, higher peak SWE, and a longer snow-covered period.

In order to evaluate the spatial modeling of snow depth, snow simulations were compared to spatially distributed snow depth observations taken during February 2011 across the STC basin. Sampling transects were located on the stubble fields and riparian forest areas near the channels. Snow is generally redistributed by wind from stubble fields to wooded areas in the Canadian Prairies (Fang & Pomeroy, 2009). The comparisons between observations and simulations indicate strong model performance. The *RMSE* for sub-basin 2 and the STC basin is 10.01 and 8.56 cm, respectively, while normalized mean bias is −0.07 and −0.05, respectively. The good model performance across a range of land uses suggests adequate representation of blowing snow erosion, transport, deposition, and in-transit sublimation (Pomeroy, Gray, & Landine, 1993). Sub-basin level water balance analyses also indicate that the sub-basin 12 which has large areas of riparian forest (Figure 4) receives a net positive blowing snow transport, while a net negative blowing snow transport was modeled in the headwater agricultural sub basins (e.g., Sub-basin 2). This inter-basin transfer of water via blowing snow has not been documented in a Canadian Prairie basin before.

TABLE 2 Snow measurement observation date, the number of snow depth observations (*N*), mean observed snow depth ($Snow\ depth_{Obs}$ in cm), and modeled snow depth ($Snow\ depth_{model}$ in cm), at the Twin basin. Note that the Twin basin mainly comprises agricultural fields

Observation date	*N*	Snow $depth_{Obs}$ (cm)	Snow $depth_{model}$ (cm)
3/9/2001	12	21	23
4/1/2001	25	14	11
2/15/2002	25	6	11
3/14/2002	25	2	0
3/12/2003	24	8	16
2/10/2004	24	26	15
3/7/2005	24	19	5
2/6/2006	23	30	37
3/7/2006	23	18	35
2/6/2007	24	18	16
3/7/2007	24	26	24
2/21/2008	24	18	20
3/17/2008	24	9	13
3/9/2009	24	25	26
3/9/2010	24	31	29
4/9/2011	31	26	28

3.2 | Flow evaluation

Table 3 provides the calculated NSE, RMSE, and normalized mean bias for daily flows for all gauges. These results demonstrate credible model capability to reproduce daily flow and temporal evolution of flows at multiple scales; however, this ability varies from year to year. Daily model performance was also good at the Hwy 240 and Miami gauges, except for during 2009 and 2011. The model performance at a daily scale was good while simulating the dry years (e.g., 2002, *NSE* = 0.7) while the model performance is weaker in wetter years (e.g., 2011, *NSE* = 0.2). However, the model performance at annual scale is adequate (*NSE* = 0.87).

Modeled streamflows were compared to observed flows at multiple scales: headwaters (sub-basin 2), mid basin (Hwy 240), and the basin outlet (Miami). Cumulative flows rather than hydrographs were compared as the intention of the model is to estimate the development of seasonal streamflows from STC rather than predict daily streamflow hydrographs. Figure 6 shows the comparisons of observed and estimated streamflow discharge for the sub-basin 2, Hwy 240, and Miami gauges. At the sub-basin 2 gauge, simulations were often in close agreement with the estimated streamflow, in particular, the model performance was good in 2001, 2002, 2003, 2005, 2006, 2009, and 2011. However, the model overestimated outflow in 2007, 2008, and 2010 at this headwater scale. Noting that daily model performance was good during the spring snowmelt runoff, the discrepancies can be attributed to inadequate spatial representation of summer rainstorm events due to lack of rain gauges in sub-basin 2. The streamflow at sub-basin 2 outlet is also influenced by a reservoir. Modeling this reservoir storage and discharge dynamics suggests that such a small reservoir barely impacts cumulative discharge. Although the reservoirs slightly lower the peak flow (0–5%), the stored water is ultimately delivered to the downstream. Thus, the very little impact is observed at the mid-basin and basin outlet scale. Overall, the modeled cumulative streamflow agrees well with observations at multiple scales, and performance improves with scale. It is assumed that measured hydrographs could be more closely matched by simulations with calibration of the lag and routing parameters but that there are limits to improvement of runoff and streamflow process representations that can be gained by calibration in this basin, due to the inadequate density of rainfall measurements. Because the sparse precipitation observations could lead to unrealistic model parameter selection by streamflow calibration, no calibration or parameter adjustments were performed.

TABLE 3 Flow simulation evaluation at multiple scales

2001–2011	*NSE* (−)	*RMSE* (mm/day)	*Normalized mean bias* (−)
Sub-basin 2 (2 km^2)	−0.1	1.44	0.33
Hwy 240 (34 km^2)	0.3	0.87	−0.04
Miami (73 km^2)	0.48	0.74	−0.02

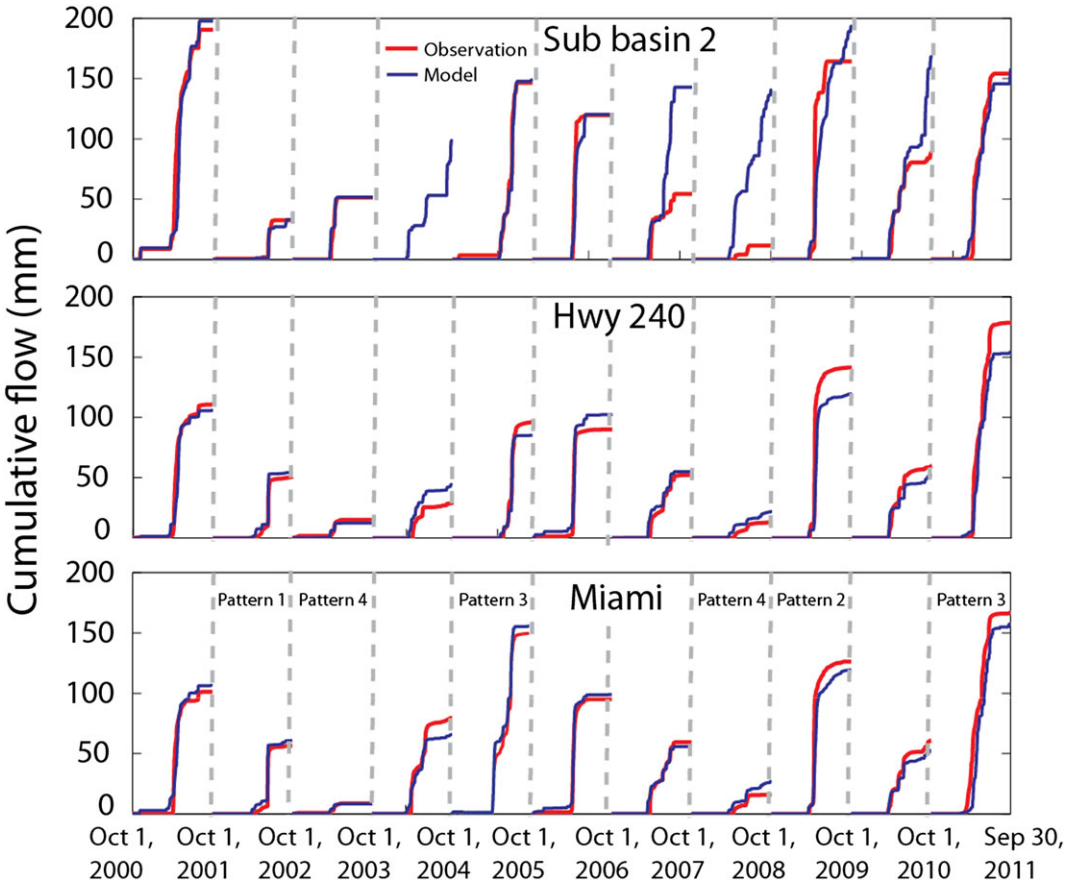

FIGURE 6 Comparisons between cumulative simulated and observed streamflow discharge at multiple scales in the South Tobacco Creek (STC) basin (2001–2011). Top, middle, and bottom figures represent streamflow comparisons at the headwater basin scale (sub-basin 2), mid-basin scale (Hwy 240), and the entire STC basin scale (Miami), respectively. Here, the simulated streamflow is shown only when the observation is available. Note that the observations during 2003–2004 period at the sub-basin 2 were not available

3.3 | Impacts of climatic variability on modeled hydrological responses

During the simulation period, the region experienced several fluctuations of precipitation regimes, whose results ranged from severe drought to record flooding. The precipitation also varied over seasons and space. Inter and intra-annual climatic variability exerted strong control on seasonal and annual modeled hydrological responses. Figure 7 shows the annual basin scale water balance including observed inputs (snowfall and rainfall), simulated outputs (snowmelt runoff, rain runoff, sublimation, drift out, and summer evapotranspiration), and simulated subsurface soil moisture storage change. In general, the STC basin showed simulated depletion of subsurface storage during the first half of the simulation period (2000–2005) which was associated with a large-scale Canadian Prairie drought (e.g., Bonsal et al., 2013). In contrast, during the second half of the

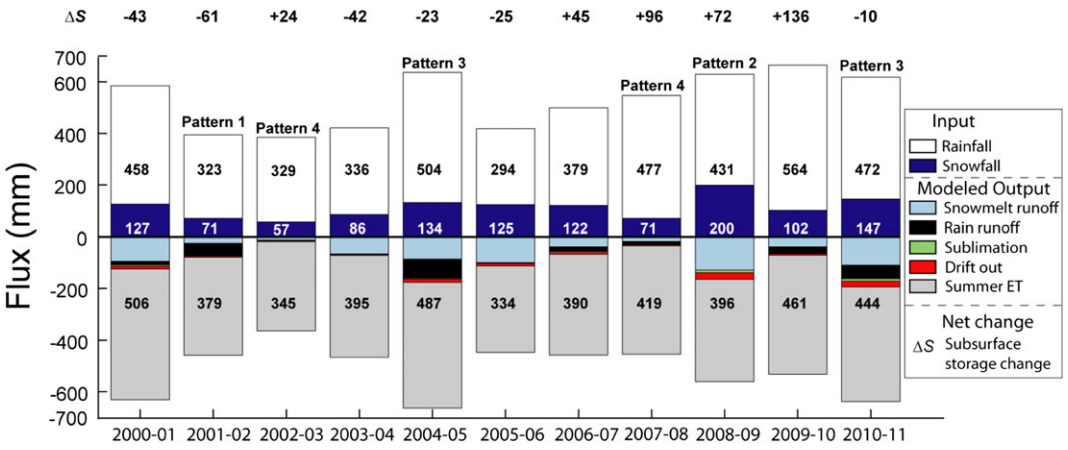

FIGURE 7 Annual simulated input and output fluxes (mm) and subsurface soil moisture storage change in the South Tobacco Creek basin over the simulation period

simulation period, addition to subsurface soil moisture storage was simulated; this can be linked to recent wetting in the eastern Canadian Prairies (e.g., Brimelow et al., 2014). Figure 7 also shows that snowmelt runoff is the major streamflow contributor to annual runoff while rainfall runoff contributions were only notable in 2001–2002, 2005–2006, and 2010–2011 (Table 4).

Figure 7 demonstrates complex hydrological patterns in response to climate variability. This study identified four major hydro-climatic patterns having unique seasonality and runoff responses, based on the four possible combinations of wet/dry winter and summer seasons. They are as follows: (1) Pattern 1: dry winter followed by wet summer (2001–2002); (2) Pattern 2: wet winter followed by dry summer (2008–2009); (3) Pattern 3 (wet years): wet year having wet winter and summer seasons (2004–2005, 2010–2011); and (4) Pattern 4 (dry years): dry year having dry winter and summer seasons (2002–2003, 2003–2004, 2007–2008). During pattern 1 (2001–2002), lower snowfall resulted in very little snowmelt runoff while a few heavy rainfall days (June 9–11, 2002) in summer generated relatively large rainfall runoff volumes. Interestingly, this rainfall runoff event was associated with extensive flooding in regions around the North Dakota–Manitoba border. However, annual runoff (70 mm) during 2001–2002 was still less than average runoff (85 mm), and simulations suggested 61 mm of water was depleted from the subsurface soil moisture storage.

In contrast, during pattern 2, heavy winter snowfall produced a large and 3-week-long snowmelt runoff event while the lack of heavy rainfall days in summer generated insignificant rainfall runoff and high summer infiltration, with simulations indicating 72 mm of subsurface soil moisture storage gain. This change in subsurface storage was primarily in the two soil layers. Note that the snowmelt runoff was also linked with 2009 spring flooding in southern Manitoba (e.g., Brimelow et al., 2014). This winter was also marked by noticeable blowing snow redistribution by wind out of the basin, smaller than normal over-winter sublimation, and markedly higher than average (127 mm) annual runoff. Pattern 3 (wet years) clearly shows greater snowmelt and rainfall runoff resulting from both heavy snowfall and frequent heavy rainfall days. In both wet years, a noticeable quantity of blowing snow transport out of the basin was simulated whereas sublimation was only notable during 2010–2011. However, in years of pattern 3 (wet years), the simulated subsurface storage experienced very little depletion due to higher evapotranspiration and higher intensity summer rainfall. The combination of wet, sometimes saturated, soils and heavy rains resulted in high runoff and little infiltration. Finally, during years of pattern 4 (dry years), lower snowfall and the lack of summer heavy rainfall days produced very little snowmelt or rainfall-runoff. Annual runoff in these years was substantially lower than the average. During pattern 4 (dry years) years, simulated subsurface soil moisture storage dynamics varied from year to year. For example, the subsurface soil moisture storage was increased by 24 mm during 2002–2003 while it was decreased by 42 mm during 2003–2004. The simulated subsurface soil moisture storage recharge in 2002–2003 can be ascribed to high infiltration capacity due to frequent, low intensity and modest volume rainfall events and to relatively low evaporative fractions. In contrast, during 2003–2004, withdrawal from subsurface soil moisture storage was modeled due to high evaporative losses in the summer season.

Others years (2000–2001, 2005–2006, 2006–2007, and 2009–2010) which were not explained by these four patterns showed unusual and contrasting water balances. For example, during 2000–2001, subsurface storage depletion from soils was due to high evapotranspiration exceeding rainfall while the highest storage recharge occurred during 2009–2010 because of large infiltration that was associated with the modest snowmelt and rainfall runoff and evapotranspiration. Infiltration (2009–2010) occurs from summer rainfall of low intensity. Surprisingly, the summer of 2010 generated very little rainfall runoff in STC whereas flooding was reported in the other parts of southern Manitoba. The summers in 2005–2006 and 2006–2007 were similar to pattern 2, but the winter snowfall was not as high. As a consequence, both years produced moderate snowmelt runoff and insignificant rainfall runoff. Interestingly, despite having similar amounts of snowfall in both years, 2005–2006 produced much higher snowmelt runoff than 2006–2007. Such contrasts can be attributed to formation of ice lenses (e.g., Gray et al., 1984; Pomeroy et al., 2007) in the frozen soils in early spring of 2006 resulting in restricted infiltration and a larger snowmelt runoff volume (see Section 3.4).

Hydroclimatic patterns in the Canadian Prairies have been previously considered, particularly in modeling studies with a strong focus on winter and spring seasons (e.g., Fang & Pomeroy, 2007; Fang &

TABLE 4 Modeled output fluxes shown in Figure 7. Fluxes include snowmelt runoff (mm), rainfall runoff (mm), sublimation (mm), drift out (mm), and ET (mm)

Year	Snowmelt runoff (mm)	Rainfall runoff (mm)	Sublimation (mm)	Drift out (mm)	ET (mm)
2000–2001	95	11	4	11	506
2001–2002	23	47	2	4	379
2002–2003	10	2	1	2	345
2003–2004	64	1	2	3	395
2004–2005	82	76	3	13	487
2005–2006	98	1	3	9	334
2006–2007	37	19	4	6	390
2007–2008	16	11	2	4	419
2008–2009	127	0	10	26	396
2009–2010	37	25	2	5	461
2010–2011	107	52	10	22	444

Pomeroy, 2008; Todhunter, 2001; Pomeroy et al., 2011). However, previous studies have considered observations over only short periods (up to 6 years) and provided very little attention to summer hydro-climatic responses. This study has identified four major hydroclimatic patterns which are difficult to observe or model because of the requirements of intensive observations and physically based simulations over long time periods. The winter hydroclimatology of pattern 1 (dry winter followed by wet summer) and pattern 4 (dry years) agrees well with those identified by Fang and Pomeroy (2007, 2008) for winter and spring-focused studies. Patterns 2 and 3 are consistent with the winter of 1997 during which large snowfall, snow accumulation, frozen soil condition, and basal ice layer lead to record flooding in the entire Red River Basin Todhunter (2001). This study adds new knowledge by incorporating summer hydroclimatic patterns and considering observations and simulations over a sufficiently long period to cover a wide range of wet and dry conditions. As a result, it has been established that a year having a dry winter does not necessarily mean dry conditions over the year, due to the importance of the subsequent summer's hydroclimate. The current study is also the first detailed hydroclimatological investigation in the Red River basin while the previous investigations were focused on drier prairie basins in Saskatchewan.

There are uncertainties in the water balance estimation from observed streamflow and driving meteorology and simulated hydrological fluxes (Figure 2; Table 4). The difference between observed and simulated annual streamflow at the basin outlet ranges from 0.05 mm (e.g., 2003) to 15 mm (e.g., 2011). The error in annual modeled streamflow is less than 5 mm during the study period with the exception of 2011 (15 mm), 2004 (12 mm), and 2008 (−11.2 mm). Furthermore, the *NSE*, *RMSE*, and *normalized mean bias* between streamflow observations and simulations at annual scale are 0.97, 7.2, and 0.0019 mm, respectively. It was not possible to evaluate other simulated water balance components such as ET due to lack of any observations. This small degree of uncertainty in streamflow simulations does not impact the findings on the four hydroclimatic patterns.

3.4 | Snowmelt runoff generation and climate variability

Figure 8a compares snowmelt runoff estimated using the simple method based on Equation 3 driven only by meteorological data with modeled snowmelt runoff using a similar algorithm but also taking into account the role of over-winter snow hydrology, for the 11 years of the simulation period. Both methods are overwhelmingly driven by snow accumulation but also strongly influenced by fall soil moisture status. However, the hydrologically modeled snowmelt runoff also takes into account basal ice layer formation beneath the snowpack and on top of frozen soils. The comparison of the simple, meteorologically driven method and the hydrologically modeled runoff in Figure 8 shows good agreement during relatively dry winters having less than 100-mm snowfall (e.g., 2002, 2003, 2007, 2008, and 2010). However, during relatively wet winters with more than 110-mm snowfall (2001, 2005, 2006, 2009, and 2011), the simple method markedly underestimates snowmelt runoff due to overestimation of snowmelt infiltration into frozen soils. This is due to the development of restricted infiltration conditions that the simple method is unable to address. Detailed diagnosis of frozen soil processes and mid-winter snowpack in the hydrological model suggests that during the wet winter years, ice lenses form due to winter and early spring thaws and rain-on-snow events. As a result, the hydrological model restricted the infiltration rate, causing a larger snowmelt runoff. Modeled SWE was also lower than observed cumulative snowfall in those winters due to blowing snow transport and sublimation losses from agricultural fields – however, this effect was overwhelmed by the impact of ice lenses. Interpretation of Figure 8a highlights the significance of land surface conditions during the snowmelt period for determining the infiltration status and consequently snowmelt runoff volume. Simulated ice lens formation years were linked with patterns 2 and 3 (Section 3.3) while ice lenses did not develop during patterns 1 and 4 years. Figure 8b shows a positive but nonlinear association between the simulated peak SWE and snowmelt runoff. Figure 8b also exhibits very little snowmelt runoff for peak SWE less than 70 mm which is also consistent with Ehsanzadeh, Spence, Van der Kamp, and McConkey (2012) calculation of no runoff for winter precipitation less than 40 mm in southwestern Saskatchewan. In both cases, infiltration to unsaturated frozen soils in dry years strongly reduces runoff as shown by Fang and

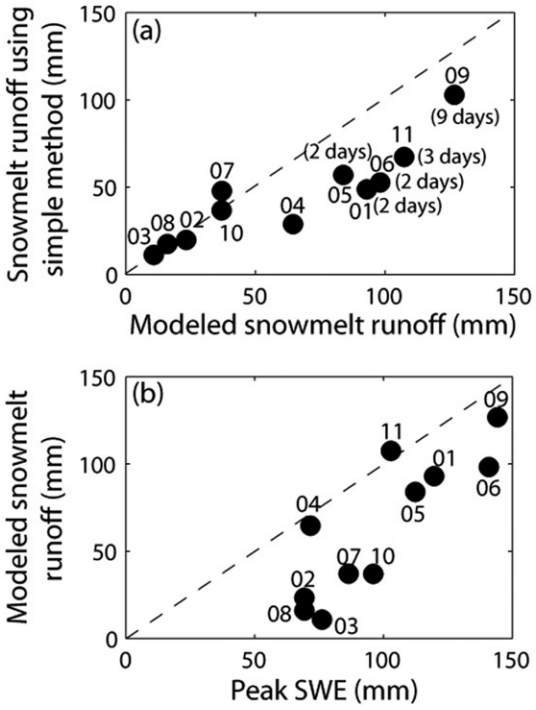

FIGURE 8 (a) Comparisons between snowmelt runoff over frozen soils estimated from Equation 1 using climate data and estimates of the CRHM model melt runoff; (b) Relationship between peak snow water equivalent (SWE) and modeled snowmelt runoff. Note that in both figures, respective years are labeled next to each black circle, for example, "08" means the 2008 winter season. However, in Figure 8a, the duration of frozen soil during snowmelt condition occurrence (i.e., basal ice layer due to mid-winter melt, unsaturated frozen soil) during the snowmelt period is indicated using text next to black circles

Pomeroy (2007), but, as shown by Gray et al. (1984, 1986), this is not a rule but is controlled by fall soil moisture content and formation of ice lenses. The snowmelt runoff is markedly lower than peak SWE during relatively dry winters (e.g., 2002, 2003, 2007, 2008, and 2010) due to high infiltration of snowmelt water. Higher infiltration is caused by lower fall soil moisture status as per the studies of Gray et al. (1984). In contrast, during relatively wet winter years (e.g., 2001, 2005, 2006, 2009, and 2011), snowmelt runoff is only slightly lower than the peak SWE, and snowmelt runoff and peak SWE are strongly correlated because of low rates of infiltration of snowmelt water. Lower rates of infiltration and higher rates of snowmelt runoff are influenced by higher fall soil moisture status and ice lens development. Figure 8b also highlights the significance of land surface state during the snowmelt period in controlling runoff volume. Based on the discussion of simulations shown in Figure 8a,b, high fall soil moisture, high peak SWE, ice lenses during the snowmelt period (Figure 8a), and restricted snowmelt infiltration are linked with patterns 2 and 3, that is, with wet winters. In contrast, low fall soil moisture, low peak SWE, absence of ice lenses, and unlimited infiltration are key characteristics for patterns 1 and 4, that is, with dry winters. In summary, snowmelt runoff is highly sensitive to both land surface conditions (i.e., ice lens development, fall soil moisture status) and peak SWE before the onset of snowmelt. It is very likely that, both winter land surface conditions and peak SWE will change as a result of climate change. These effects of climate change may be particularly marked during wet (patterns 2 and 3) winters (e.g., Rasouli et al., 2014).

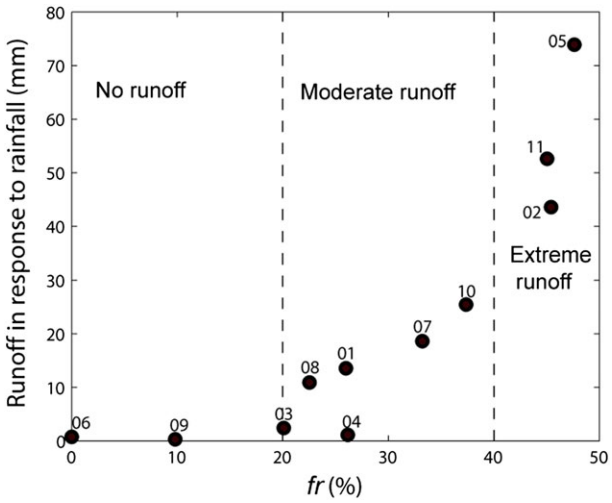

FIGURE 9 Cross plot between *fr* (%) and rainfall runoff in the South Tobacco Creek basin. Note that *fr* (%) is defined as the fractional contribution of summer rainfall by heavy rainfall days (25 mm/day). The text next to each black circle indicates the year, for example, "08" means the 2008 summer season

3.5 | Rainfall runoff generation

Rainfall runoff generation at STC is related to the frequency and intensity of heavy rainfall days and has no relationship with annual rainfall volume. Figure 9 clearly shows that a larger proportional contribution by heavy rainfall days (≥25 mm/day) to seasonal rainfall depth (*fr*) produces more rainfall runoff. However, the relationship between *fr* and seasonal rainfall runoff volume is nonlinear and shows thresholding behavior. Its nonlinearity provides valuable insights into the relationship between *fr* and runoff generation. When *fr* was less than 20%, no rainfall runoff was generated. Above 20% *fr*, a threshold is crossed where there is now runoff generation, and for 20% > *fr* < 40%, a linear relationship between *fr* and runoff volume developed. However, when *fr* > ~40%, then runoff volume became independent of *fr*. Here, additional high temporal resolution rainfall observations (hourly or sub-daily) might be useful to explain the rainfall runoff generation for higher *fr*. Table 5 provides rainfall event characteristics producing significant runoff volumes from hourly rainfall data collected by the Twin sub-basin gauge and indicates storms of more than 18 hr with a least a few hours of high-intensity rainfall storms that are required to generate significant rainfall-runoff at the basin scale. This is because longer duration events have greater spatial coverage and with the sparse STC rainfall gauging network the only way to infer that a large rainfall volume is received by the basin is to observe a long duration and high rate of rainfall at a gauge. For example, in 2002, a significant rainfall event of 164 mm over 52 hr, with >10 mm rainfall per hour for 5 hr, produced 99% of the rainfall runoff and 71% of the annual runoff. Higher spatial and temporal resolution of rainfall measurements would be very useful to better predict runoff in response to rainfall. Finally, it can be concluded that for the years with a very high fraction or very low fraction of heavy rainfall days, the rainfall runoff volume is independent of *fr*. Very low *fr* values are linked with summer drought years (pattern 4, pattern 2), and very high *fr* values are associated with wet summer years (pattern 1 and pattern 3). The unsaturated infiltration rates into prairie soils are greater than all but the more extreme rainfall rates. It is possible therefore that restricted infiltration is due to the heavy texture and slow drainage of Red River Basin soils, which promotes the development of a transient saturated layer perched on glacial till in wet conditions such as during a large rainstorm. This combination of extreme rainfall with a perched saturated soil layer can generate runoff during the summer season.

TABLE 5 Characteristics of major summer rainfall events that generated substantial rainfall runoff

Event date	Duration (h)	Max rate (mm/h)	# of hours > 10 mm/hr	Total rainfall (mm)	Basin wide rainfall variation (mm)	Total runoff at Miami (mm)
June 9–11, 2002	52	19.25	5	164	128–200	50
June 29–30, 2005	18	16.32	3	74	65–88	34
May 21, 2011	24	8.32	0	60	Not available	12

4 | CONCLUSIONS

Climatic variability, manifested through seasonality as sequences of wet and dry winters and summers, was found to exert strong controls on hydrological responses in Canadian Prairie agricultural basins. Using a physically based, distributed cold regions hydrological model, the effects of this interannual climatic variability were assessed in a medium-sized Manitoba agricultural basin over an 11-year period characterized by dry and wet years. This is believed to be the first uncalibrated, physically based hydrological model application in southern Manitoba. The model was able to reproduce both snow depth and SWE observations at the seasonal scale and, on an annual basis, streamflow observations at multiple scales in the STC basin, and the model performance was adequate for capturing the spatiotemporal dynamics of observations at larger scales.

Following the model setup and performance evaluation, detailed investigations identified four seasonal hydro-climatic patterns affecting rainfall and snowmelt runoff generation:

Pattern 1. (wet summer after dry winter): low snowmelt runoff, high rainfall runoff, below average annual runoff, high contribution of heavy rainfall days (≥25 mm/day) to seasonal rainfall depth (*fr*), low winter snowfall, and substantial subsurface soil moisture storage depletion.

Pattern 2. (dry summer after wet winter): heavy winter snowfall, significant volume of snowmelt runoff lasting for few weeks, over-winter ice lenses forming and restricting infiltration during snowmelt, blowing snow transport out of the basin, low rainfall runoff, low *fr*, above average annual runoff, and substantial subsurface soil moisture storage gains.

Pattern 3. (wet winter and summer): high snowmelt and rainfall runoff due to high winter snowfall and high *fr*, over-winter ice lense formation restricting infiltration during snowmelt, above average annual runoff, blowing snow transport from the basin, and slight depletion in subsurface soil moisture storage.

Pattern 4. (dry winter and summer): low snowmelt and rainfall runoff due to smaller snowfall and low *fr*. Variable subsurface soil moisture storage dynamics which depended on rainfall runoff volumes. The findings during the drought years (pattern 4) are supported by previous scientific studies (e.g., Fang & Pomeroy, 2007; Fang & Pomeroy, 2008).

The hydro-climatic patterns identified have useful implications for anticipating future hydrological responses in southern Manitoba. Bonsal et al. (2013) projected greater drought frequency and severity using the Palmer Drought Sensitivity Index and higher perseverance of multi-year drought using standardized precipitation index in the southern prairies. The Palmer Drought Sensitivity Index-based scenario can easily be linked with pattern 4 to predict future runoff responses. Further, the standardized precipitation index-based scenario is more comparable to the multi-year dry period (2002–2004). Sushama, Khaliq, and Laprise (2010) examined future drought characteristics using a Canadian Regional Climate Model and predicted an increased number of dry days and longer dry spell duration (April–September) as well as greater occurrence of heavy rainfall days over the southern prairies. Such a scenario is comparable to the summers having high *fr* values as seen in 2002.

Patterns 1 and 2 are years with "contrary extremes" that have an inverse relationship between seasonal runoff responses which has major implications for the prairie economy because both patterns are linked with extensive flooding. In this study, an extreme rainfall runoff event during pattern 1 year was coincident with summer flooding (early June) that was devastating for regional agriculture. In contrast, a massive spring snowmelt runoff event was also concurrent with spring flooding during pattern 2 year, resulting in significant damage. However, the following summer after spring flooding was very dry. As a consequence, some farmers in southern Manitoba filed both flood and drought insurance claims for the 2009 growing season (Government of Manitoba, 2012). These results showing contrary extremes in seasonal hydro-climatic responses are useful for predicting hydrological responses and risk of natural disasters.

The fractional percentage of heavy rainfall days in summer seasons (*fr*) was helpful to understand differences in runoff volume and key thresholding behavior. Summers having low *fr* generated no rainfall runoff whilst the summers with high *fr* produced extreme rainfall runoff volumes. However, high temporal resolution (e.g., hourly or sub-hourly) rainfall data are needed for improving understanding of runoff generation during wet summers because runoff generation depends on rainfall rate rather than total rainfall volume.

The comparison between a snow hydrology model and a simple implementation of a snowmelt infiltration to frozen soil equation from meteorological data (Granger et al., 1984) clearly illustrated the importance of considering ice lens formation as a driver of increasing snowmelt runoff and the role of blowing snow ablation in modifying snowmelt runoff during wet winter years. High snow accumulation does not necessarily mean high spring runoff but also requires a wet preceding fall to restrict infiltration to frozen soils and is enhanced by winter and early spring thaws or rain-on-snow events that cause basal ice layer formation between the snowpack and frozen ground. Warmer climates in the future are expected to influence snow accumulation, ice lens formation, restricted infiltration, and snowmelt timing. The impacts of warmer winters may reduce the frequency and likelihood of ice lens formation during snowmelt, which may increase snowmelt infiltration and lessen snowmelt runoff in the wet winters of patterns 2 and 3 years (Dumanski, Pomeroy, & Westbrook, 2015; Rasouli et al., 2014).

Spring snowmelt and summer rainfall runoff are both contributors to annual runoff in the basin, but their contributions differ markedly from year to year. Snowmelt runoff production depends primarily on winter snowfall, infiltration status during the snowmelt period, and ablation of blowing snow. In contrast, rainfall runoff generation relies on summer *fr*, duration of rainfall event, and rainfall rate. These indirectly control summer infiltrability and the ability to generate overland flow. Snowmelt runoff is the more reliable and stable source of prairie annual runoff while the rainfall runoff contribution fluctuates greatly from year to year depending on the intensity and duration of rainfall storms (Dumanski et al., 2015).

There are important implications for water quality. Nutrient export is altered by land use in this basin and also by hydrological and climatic factors (Liu et al., 2014a). Within the Lake Winnipeg Basin, increases in

flows and in particular in flooding are hypothesized to be a major driver of the recent increase in phosphorus loads associated with eutrophication (McCullough et al., 2012). The physically based modeling results reported here demonstrate that winter snowfall, infiltration status during snowmelt, and snow redistribution can play key roles in determining flows and, as such, are likely to affect nutrient loads (Corriveau, Chambers, & Culp, 2013). Rainfall runoff can also be an important mode of nutrient transport in this basin, and findings here suggest that high-resolution rainfall observations and additional streamflow observations at distributed locations would be beneficial in simulations of rainfall runoff and catchment-scale simulations of nutrient export. In addition to rainfall and streamflow gauges, other observations such as soil moisture, SWE, evapotranspiration, soil temperature, groundwater observations (installations of more wells), and distributed soil hydraulic properties are strongly recommended to improve our process understandings and numerical simulations.

ACKNOWLEDGMENTS

We would like to thank Agriculture and Agri-Food Canada, Environment and Climate Change Canada, and Deerwood Soil and Water Management Association for providing datasets. We would also like to thank Canada Water Network, Global Institute of Water Security and NSF funded ND EPSCoR (NSF grant #IIA-135466) for funding the current research. Finally, special thanks to Jane Elliott, Tom Brown, Xing Fang, Les McEwan, and Don Cruikshank for providing data set and assisting with modeling.

REFERENCES

Annandale, J. G., Jovanic, N. Z., Benade, N., & Allen, R. G. (2002). Software for missing data error analysis of Penman-Monteith reference evapotranspiration. *Irrigation Science*, *21*, 57–67.

Armstrong, R. N., Pomeroy, J. W., & Martz, L. W. (2008). Evaluation of three evaporation estimation methods in a Canadian prairie landscape. *Hydrological Processes*, *22*, 2801–2815.

Armstrong, R. N., Pomeroy, J. W., & Martz, L. W. (2010). Estimating evaporation in a Prairie landscape under drought conditions. *Canadian Water Resources Journal*, *35*, 173–186.

Armstrong, R. N., Pomeroy, J. W., & Martz, L. W. (2015). Variability in evaporation across the Canadian Prairie region during drought and non-drought periods. *Journal of Hydrology*, *521*, 182–195.

Ayers HD. (1959). Influence of soil profile and vegetation characteristics on net rainfall supply to Runoff. In *Proceedings of Hydrology Symposium No.1: Spillway Design Floods*, National Research Council Canada: Ottawa; 198–205.

Bonsal, B. R., & Lawford, R. (1999). Teleconnections between El Niño and La Niña events and summer extended dry spells on the Canadian Prairies. *International Journal of Climatology*, *19*, 1445–1458.

Bonsal, B. R., & Wheaton, E. E. (2005). Atmospheric circulation comparison between the 2001 and 2002 and the 1961 and 1988 Canadian Prairie droughts. *Atmosphere–Ocean*, *4*, 163–172.

Bonsal, B. R., Wheaton, E. E., Chipanshi, A., Lin, C., Sauchyn, D. J., & Wen, L. (2011a). Drought research in Canada: a review. *Atmosphere–Ocean*, *49*, 303–319.

Bonsal, B. R., Wheaton, E. E., Meinert, A., & Siemens, E. (2011b). Characterizing the surface dynamics of the 1999–2005 Canadian Prairie drought in relation to previous severe 20th century events. *Atmosphere–Ocean*, *49*, 320–338.

Bonsal, B. R., Aider, R., Gachon, P., & Lapp, S. (2013). An assessment of Canadian prairie drought: past, present and future. *Climate Dynamics*, *41*(2), 501–516. doi:10.1007/s00382-012-1422-0

Brimelow, J. C., Raddatz, R. L., & Hayashi, M. (2010a). Validation of ET estimates from the Canadian Prairie agrometeorological model for contrasting vegetation types and growing seasons. *Canadian Water Resources Journal*, *35*(2), 209–230.

Brimelow, J. C., Hanesiak, J. M., & Raddatz, R. L. (2010b). Validation of soil moisture simulations from the PAMII model, and an assessment of their sensitivity to uncertainties in soil hydraulic parameters. *Agricultural and Forest Meteorology*, *150*, 100–114.

Brimelow, J. C., & Hanesiak, J. M. (2011). Validation of modelled soil moisture and evapotranspiration from the PAMII model, and an assesment of their utility for tracking drought. In R. Stewart, & R. Lawford (Eds.), *The 1999–2005 Canadian Prairies Drought: Science, Impact, and Lessons*. (pp. 114). Winnipeg: MB.

Brimelow, J. C., Stewart, R. E., Hanesiak, J. M., Kochtubajda, B., Szeto, K., & Bonsal, B. R. (2014). Characterization and assessment of the devastating natural hazards across the Canadian Prairie Provinces from 2009 to 2011. *Natural Hazards*, *73*, 761–785.

Chow, V. T., Maidment, D. R., & Mays, L. W. (1988). *Applied Hydrology*. (pp. 572). Toronto: Tata McGraw-Hill Education (reprint edition).

Corriveau, J., Chambers, P. A., & Culp, J. M. (2013). Seasonal variation in nutrient export along streams in the Northern Great Plains. *Water, Air, and Soil Pollution*, *224*, 1594. doi:10.1007/s11270-013-1594-1

Dornes, P. F., Pomeroy, J. W., Pietroniro, A., Carey, S. K., & Quinton, W. L. (2008). Influence of landscape aggregation in modelling snow-cover ablation and snowmelt runoff in a sub-arctic mountainous environment. *Hydrological Sciences Journal*, *53*, 725–740.

Dumanski, S., Pomeroy, J. W., & Westbrook, C. J. (2015). Hydrological regime changes in a Canadian Prairie basin. *Hydrological Processes*, *29*, 3893–3904. doi:10.1002/hyp.10567

Ehsanzadeh, E., Spence, C., Van der Kamp, G., & McConkey, B. (2012). On the behaviour of dynamic contributing areas and flood frequency curves in North American Prairie watersheds. *Journal of Hydrology*, *414-415*, 364–373.

Ellis, C. R., & Pomeroy, J. W. (2007). Estimating sub-canopy shortwave irradiance to melting snow on forested slopes. *Hydrological Processes*, *21*, 2581–2593. doi:10.1002/hyp.6794

Ellis, C. R., Pomeroy, J. W., Brown, T., & MacDonald, J. (2010). Simulation of snow accumulation and melt in needleleaf forest environments. *Hydrology and Earth System Sciences*, *14*, 925–940. doi:10.5194/hess-14-925-2010

Fang X, Pomeroy JW. (2007). Snowmelt runoff sensitivity analysis to drought on the Canadian Prairies. *Hydrological Processes*, *21*: 2594–2609, doi:10.1002/hyp.6796

Fang, X., & Pomeroy, J. W. (2008). Drought impacts on Canadian prairie wetland snow hydrology. *Hydrological Processes*, *22*(15), 2858–2873 . doi:10.1002/hyp.6796

Fang, X., & Pomeroy, J. W. (2009). Modelling blowing snow redistribution to prairie wetlands. *Hydrological Processes*, *23*, 2557–2569.

Fang, X., Pomeroy, J. W., Westbrook, C. J., Guo, X., Minke, A. G., & Brown, T. (2010). Prediction of snowmelt derived streamflow in a wetland dominated prairie basin. *Hydrology and Earth System Sciences*, *14*, 991–1006. doi:10.5194/hess-14-991-2010

Fang, X., Pomeroy, J. W., Ellis, C. R., MacDonald, M. K., DeBeer, C. M., & Brown, T. (2013). Multi-variable evaluation of hydrological model predictions for a headwater basin in the Canadian Rocky Mountains. *Hydrology and Earth System Sciences*, *17*, 1635–1659. doi:10.5194/hess-17-1635-2013

Garnier, B. J., & Ohmura, A. (1970). The evaluation of surface variations in solar radiation income. *Solar Energy*, *13*, 21–34.

Government of Manitoba, (2009). Manitoba 2009 spring flood report. http://www.gov.mb.ca/waterstewardship/reports/floods/spring_flood_2009.pdf Accessed Jun 2, 2015.

Government of Manitoba, (2012). http://news.gov.mb.ca/news/index.html?archive=2012-11-01&item = 15561. Accessed 25 Jan 2013

Granger, R. J., Gray, D. M., & Dyck, G. E. (1984). Snowmelt infiltration to frozen Prairie soils. *Canadian Journal of Earth Sciences*, *21*, 669–677.

Granger, R. J., & Gray, D. M. (1990). A new radiation model for calculating daily snowmelt in open Environments. *Nordic Hydrology*, *21*, 217–234.

Gray, D. M., Dyck, G. E., & Granger, R. J. (1984). Snowmelt Infiltration to frozen Prairie Soils. *Canadian Journal of Earth Sciences*, *21*, 669–677.

Gray DM, Pomeroy JW, Granger RJ. (1986). Prairie snowmelt runoff. *Proceedings, Water Research Themes, Conference Commemorating the Official Opening of the National Hydrology Research Centre*. Canadian Water Resources Association: Saskatoon; 49–68.

Gray, D. M., & Landine, P. G. (1987). Albedo model for shallow prairie snow covers. *Canadian Journal of Earth Sciences*, *24*, 1760–1768.

Jarvis, P. G. (1976). The interpretation of the variations in leaf water potential and stomatal conductance found in canopies in the field. *Philosophical Transactions of the Royal Society of London SeriesB-Biological Sciences*, *273*, 593–610 .A Discussion on Water Relations of Plants

Jenson, S. K., & Domingue, J. O. (1988). Extracting topographic structure from digital elevation data for geographic information system analysis. *Photogrammetric Engineering and Remote Sensing*, *54*, 1593–1600.

Koiter, A. J., Lobb, D. A., Owens, P. N., Petticrew, E. L., Tiessen, K. H. D., & Li, S. (2013). Investigating the role of connectivity and scale in assessing the sources of sediment in an agricultural watershed in the Canadian prairies using sediment source fingerprinting. *Journal of Soils and Sediments*, *13*, 1676–1691.

Liu, J., Stewart, R. E., & Szetco, K. K. (2004). Moisture transport and other hydrometeorological features associated with the severe 2000/01 drought over the western and central Canadian Prairies. *Journal of Climate*, *17*, 305–319.

Liu, K., Elliott, J. A., Lobb, D. A., Flaten, D. N., & Yarotski, J. (2014a). Critical factors affecting field-scale losses of nitrogen and phosphorus in spring snowmelt runoff in the Canadian prairies. *Journal of Environmental Quality*, *42*, 484–496.

Liu, Y., Yang, W., Yu, Z., Lung, I., Yarotski, J., Elliott, J., & Tiessen, K. (2014b). Assessing effects of small dams on stream flow and water quality in an agricultural watershed. *Journal of Hydrologic Engineering*, *19*, doi: 10.1061/(ASCE)HE.1943-5584.0001005, 05014015.

Liu, Y., Yang, W., Yu, Z., Lung, I., & Gharabaghi, B. (2015). Estimating sediment yield from upland and channel erosion at a watershed scale using SWAT. *Water Resources Management*, *29*, 1399–1412.

Lopez-Moreno, J. I., Pomeroy, J. W., Revuelto, J., & Vicente-Serrano, S. M. (2012). Response of snow processes to climate change: spatial variability in a small basin in the Spanish Pyrenees. *Hydrological Processes*, *27*, 2637–2650. doi:10.1002/hyp.9408

Marin, S., van der Kamp, G., Pietroniro, A., Davison, B., & Toth, B. (2010). Use of geological weighing lysimeters to calibrate a distributed hydrological model for the simulation of land–atmosphere moisture exchange. *Journal of Hydrology*, *383*, 179–185.

McCullough, G. K., Page, S. J., Hesslein, R. H., Stainton, M. P., Kling, H. J., Salki, A. G., & Barber, D. G. (2012). Hydrological forcing of a recent trophic upsurge in Lake Winnipeg. *Journal of Great Lakes Research*, *38*, 95–105.

Monteith, J. L. (1965). Evaporation and environment. *Symposia of the Society for Experimental Biology*, *19*, 205–224.

Nash, J. E., & Sutcliffe, J. V. (1970). River flow forecasting through conceptual models part I—a discussion of principles. *Journal of Hydrology*, *10*, 282–290.

Nkemdirim, L., & Weber, L. (1999). Comparison between the droughts of the 1930s and the 1980s in the southern Prairies of Canada. *Journal of Climate*, *12*, 2434–2450.

Pomeroy, J. W., Gray, D. M., & Landine, P. G. (1993). The Prairie Blowing Snow Model: characteristics, validation, operation. *Journal of Hydrology*, *144*, 165–192.

Pomeroy, J. W., & Li, L. (2000). Prairie and arctic areal snow cover mass balance using a blowing snow model. *Journal of Geophysical Research*, *105*, 26619–26634.

Pomeroy, J. W., Gray, D. M., Brown, T., Hedstrom, N. R., Quinton, W., Granger, R. J., & Carey, S. (2007). The cold regions hydrological model, a platform for basing process representation and model structure on physical evidence. *Hydrological Processes*, *21*, 2650–2667. doi: 10.1002/hyp.6787

Pomeroy, J. W., Marks, D., Link, T. E., Ellis, C. R., Hardy, J., Rowlands, A., & Granger, R. J. (2009). The impact of coniferous forest temperature on incoming longwave radiation to melting snow. *Hydrological Processes*, *23*, 2513–2525.

Pomeroy, J. W., Pietroniro, A., Fang, X., Shaw, D., Armstrong, R., Shook, K., … Westbrook, C. (2011). Canadian prairie drought hydrology. In R. Stewart, & R. Lawford (Eds.), *The 1999–2005 Canadian Prairies Drought: Science, Impact, and Lessons*. (pp. 114). Winnipeg: MB.

Pomeroy, J. W., Fang, X., Shook, K., & Whitfield, P. H. (2013). Predicting in ungauged basins using physical principles obtained using the deductive, inductive, and abductive reasoning approach. In *Putting Prediction in Ungauged Basins into Practice*. (pp. 41–61). Canada: Canadian Water Resources Association.

Raddatz, R. L. (2000). Summer rainfall recycling for an agricultural region of the Canadian prairies. *Canadian Journal of Soil Science*, *80*, 367–373.

Rasouli, K., Pomeroy, J. W., Janowicz, J. R., Carey, S. K., & Williams, T. J. (2014). Hydrological sensitivity of a northern mountain basin to climate change. *Hydrological Processes*, *28*, 4191–4208.

Roberts, E., Stewart, R. E., & Lin, C. L. (2006). A study of drought characteristics over the Canadian prairies. *Atmosphere–Ocean*, *44*(4), 331–345. doi:10.3137/ao.440402

Sushama, L., Khaliq, N., & Laprise, R. (2010). Dry spell characteristics over Canada in a changing climate as simulated by the Canadian RCM. *Global and Planetary Change*, *74*, 1–14.

Shabbar, A., Bonsal, B. R., & Khandekar, M. (1997). Canadian precipitation patterns associated with the Southern Oscillation. *Journal of Climate*, *10*, 3016–3027.

Shabbar, A., Bonsal, B. R., & Szeto, K. (2011). Atmospheric and oceanic variability associated with growing season droughts and pluvials on the Canadian Prairies. *Atmosphere–Ocean*, *49*, 339–355.

Shook, K., & Pomeroy, J. W. (2012). Changes in the hydrological character of rainfall on the Canadian prairies. *Hydrological Processes*, *26*, 1752–1766.

Sicart, J. E., Pomeroy, J. W., Essery, R. L. H., & Bewley, D. (2006). Incoming longwave radiation to melting snow: observations, sensitivity and estimation in northern environments. *HydrologicalProcesses*, *20*, 3697–3708. doi:10.1002/hyp.6383

Stewart, R. E., Henson, W., Carmichael, H., Hanesiak, J., & Szetco, K. (2011). Precipitation events during the recent drought. In R. Stewart, & R. Lawford (Eds.), *The 1999–2005 Canadian Prairies Drought: Science, Impact, and Lessons*. (pp. 114). Winnipeg: MB.

Stewart, R. E., Bonsal, B. R., Harder, P., Henson, W., & Kochtubajda, B. (2014). Cold and hot periods associated with dry conditions over the Canadian prairies. *Atmosphere–Ocean*, *50*(3), 364–372.

Tarboton, D. G., Bras, R. L., & Rodriguez–Iturbe, I. (1991). On the extraction of channel networks from digital elevation data. *Hydrological Processes*, *5*, 81–100.

Tiessen, K. H. D., Elliott, J. A., Yarotski, J., Lobb, D. A., Flaten, D. N., & Glozier, N. E. (2010). Conventional and conservation tillage—influence on seasonal runoff, sediment and nutrient losses in the Canadian Prairies. *Journal of Environmental Quality*, *39*, 964–980.

Tiessen, K. H. D., Elliott, J. A., Stainton, J., Yarotski, J., Flaten, D. N., & Lobb, D. A. (2011). The effectiveness of small-scale headwater storage dams and reservoirs on stream water quality and quantity in the Canadian Prairies. *Journal of Environmental Quality*, *66*, 158–171.

Todhunter, P. E. (2001). A hydroclimatological analysis of the Red River of the north snowmelt flood catastrophe of 1997. *Journal of the American Water Resources Association*, *37*, 1263–1278.

Van der Kamp, G., & Hayashi, M. (2001). The response of groundwater levels, wetlands and lakes in western Canada to drought. In R. Stewart, & R. Lawford (Eds.), *The 1999–2005 Canadian Prairies Drought: Science, Impact, and Lessons*. (pp. 114). Winnepeg: MB.

Verseghy, D. L. (1991). CLASS – a Canadian land surface scheme for GCMs, I. Soilmodel. *International Journal of Climatology*, *11*, 111–133.

Verseghy, D. L., McFarlane, N. A., & Lazare, M. (1993). A Canadian land surface scheme for GCMs: II. Vegetation model and coupled runs. *International Journal of Climatology*, *13*, 347–370.

Yang, W., Rousseau, A. N., & Boxall, P. (2007). An integrated economic-hydrologic modeling framework for the watershed evaluation of beneficial management practices. *Journal of Soil and Water Conservation*, *62*, 423–432.

Yarotski J, Rickwood, R. (2004). Meteorological and runoff data for 2003 collected in the south Tobacco Creek Basin near Miami, Manitoba. Agriculture and Agro-food Canada, Regina, 40p.

Yarotski J, Rickwood, R. (2007). Meteorological and runoff data for 2006 collected in the south Tobacco Creek Basin near Miami, Manitoba. Agriculture and Agro-food Canada, Regina, 82p.

How to cite this article: Mahmood, T. H., Pomeroy, J. W., Wheater, H. S., and Baulch, H. M. (2016), Hydrological responses to climatic variability in a cold agricultural region, *Hydrological Processes*, doi: 10.1002/hyp.11064